

Development of Cloud Computing System for Concrete Structure Inspection by Deep Learning Based Infrared Thermography Method

Shogo Hayashi ^a and Koichi Kawanishi ^b and Isao Ujike ^c and Pang-Jo Chun ^d

^{a b} West Nippon Expressway Engineering Shikoku Company Limited, Takamatsu, Japan

^c Ehime University, Matsuyama, Japan

^d The University of Tokyo, Tokyo, Japan

E-mail: shogo.hayashi@w-e-shikoku.co.jp, koichi.kawanishi@w-e-shikoku.co.jp, iujike@cee.ehime-u.ac.jp,
iujike@cee.ehime-u.ac.jp, chun@g.ecc.u-tokyo.ac.jp

Abstract –

In recent years, deterioration of concrete structures such as floating and delamination has occurred. These damages can lead to the falling of concrete pieces. It may cause damage to third parties such as vehicles or pedestrians passing under the bridge. Therefore, the concrete damages need to be detected and repaired early.

Japanese highway companies conduct hammering tests on concrete structures once every five years to detect damages such as floating and flaking. However, the inspector must be near the bridge to perform the hammering sound inspection, which requires work at a high place and a lot of time and cost. Also, when using aerial work vehicles, traffic regulation under the bridge is required which may cause traffic congestion and accidents.

Infrared thermography is a non-destructive inspection technique that detects areas of floating or delamination by imaging a unique temperature distribution on the concrete surface using an infrared camera. The inspection cost of infrared thermography is significantly lower than that of hammering test. Since it is a long-distance non-destructive inspection, work at heights and traffic restrictions are not required. However, it is difficult to ensure the accuracy of damage detection because the peculiar temperature distribution acquired by infrared thermography includes an abnormal temperature distribution caused by something other than damages.

In this study, by using deep learning, we improved the accuracy of the unique temperature distribution imaged by infrared thermography and ensured detection accuracy that can be used practically. We also report on the construction of an

automatic discrimination system that implements the deep learning discrimination algorithm on a cloud server.

Keywords –

Deep Learning; Infrared Thermography; Cloud Computing System

1 Introduction

Aging of concrete structures has been escalating recently, and there have been several reports of concrete piece falling accidents due to fractures of PC reinforcement rods and PC stranded wire in prestressed concrete, or corrosion of reinforcement steel rods. For instance, On April 3, 2009, the cover concrete with a length of 1 m, a width of 100 mm, a thickness of 260 mm, and a weight of 6 kg fell due to the corrosion of the rebar installed in the drainage unit of Tooridani bridge in Shikokuchuo-city. If flaky concrete hits a passer-by, it can cause a secondary disaster, so such accidents should be prevented as much as possible.

Several nondestructive inspection (NDI) techniques are available for the task [1][2]. In our project, we have decided to establish a detection technique of areas with floating and delamination based on the passive infrared thermography method, which would not limit the target bridges and should be able to inspect the target remotely and entirely.

The infrared thermography method has already been applied in the detection of floating of building tiles, but currently, it has not been applied to the inspection of floating and delamination of the concrete structures that have been put to practical use[4][5]. That's because the detection rate is significantly lower than conventional hammering tests. To enhance the detection rate, we first

examined infrared cameras by comparing their performances. As a result, the most suitable type was a cooling type camera, which has a shorter measurement wavelength range. We also developed a method to analyze the acquired thermal images and detect damages thoroughly. Specifically, it enables the machine to detect damages through machine learning, which has learned both anomalous forms in the areas of temperature alteration and the texture within the target areas.

2 EQUIPMENT AND METHOD OF INSPECTION

2.1 Equipment

ASTM D 4788 (Standard Test Method for Detecting Delaminations in Bridge Decks Using Infrared Thermography) requires the following conditions in thermal imaging [3].

- 1) Targets that are in constant contact with water, ice, or snow should not be applicable for shooting; they must be dried at least for 24 hours.
- 2) The condition with over 25 km/h wind velocity should not be applicable for shooting.
- 3) Thermal imaging at night should be taken in fine weather.

It also requires specific weather criteria for shooting as shown in the following table.

Table 1. The weather criteria for thermal imaging.

The weather condition of two hours before the test start	Determination
Fair	Possible
Fair with occasional clouds	Possible
Cloudy with occasional fine weather	Possible
Cloudy with temporary fine weather	Impossible
Cloudy	Impossible
Rain	Impossible

It is also critical to select the right infrared camera to get accurate detection results. Some of the essential specifications for an infrared camera should be its pixel resolution, detecting element, measurement wavelength, noise equivalent temperature difference (NETD), or frame rates, in which NETD is the most important. Regarding NETD, the infrared camera candidates we evaluated for our investigation were roughly classified into two groups; 0.02°C-NETD and 0.06°C-NETD. To determine the selection criteria for the thermal camera, we need to confirm the temperature difference in the target floating/delamination areas. Considering the fact

that the typical cover of the bridge's upper structure is 40mm, it is essential to select the camera capable of detecting cracks and voids 40mm below the surface. We built some model structures to investigate thermal cameras' detection capability and weather conditions and selected one that could detect the cracks and the voids 40 mm below.

2.1.1 Building Model Structures and Photographing Conditions

We built cubic concrete model structures. Each model has a void with the size of 100mm x 100mm ($t=10\text{mm}$) in a different depth from the surface; 20mm, 30mm, 40mm, and 60mm, respectively (Fig. 1). In order to avoid the influence of daytime sunshine, a model was installed in the shade under the bridge on the Takamatsu Expressway and photographed at night (23:00) under weather conditions with a daily difference of 10°C or more.

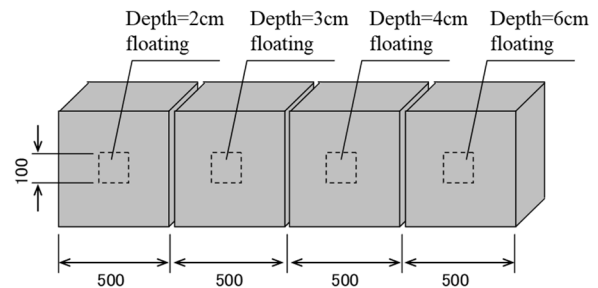


Figure 1. Concrete model structures and locations of voids.

2.1.2 Thermal Images of Each Infrared Camera

We used three cameras with different measurement wavelength and NETD in photographing model structures. We set two cameras of different NETD in line and photographed model structures simultaneously. Photographing with the camera of the minimum thermal sensitivity below 0.06°C could not detect the void. The thermal images of the camera with minimum thermal sensitivity of 0.025°C or less succeeded in detecting the void up to the depth of 40mm. We also learned that even the camera with below 0.025°C minimum thermal sensitivity could not detect the void in 60mm deep, due to signal-to-noise ratio (SNR) of the camera. The result suggests that the camera with minimum thermal sensitivity below 0.025°C is applicable for inspection of the upper structure, but not for lower structures with much thicker covers.

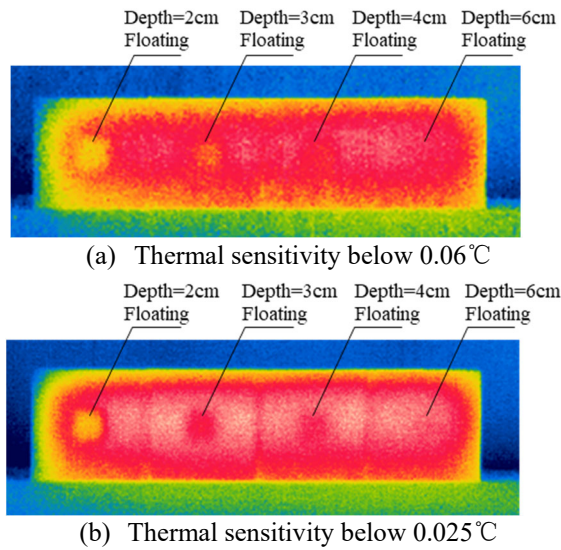


Figure 2. Thermal images of concrete model structure

2.2 Thermal Environment Suitable for Infrared Thermography Method

The infrared thermography method requires the generation and the retention of heat flow inside the target object for several hours. Usually, Equation 1 should calculate the required time for the operation. However, due to heat transmission from the area around the target, it takes longer than the time derived from Equation 1 before the surface temperature of the floating/delamination area changes. In our experiment, the temperature change appeared in the condition with 2°C difference continuously for an hour between object and air temperatures.

$$d = 2\sqrt{\frac{\lambda t}{\rho c}}$$

where

d : Heat transmission depth (m)

λ : Heat conductivity (W/mk)

t : Time of appearance (sec)

ρ : Density (kg/m³)

c : Specific heat (J/kg K)

(1)

3 3 EXAMINATION OF THERMAL IMAGE ANALYSIS METHOD

3.1 Necessity and outline of the thermal image analysis method

Some of the problems with infrared thermography measurements are the risk of overlooking and false detection of floating and delaminations by inspection

personnel. Therefore, we have built an automatic detection system for floating and delamination based on machine learning.

However, the analysis requires preprocessing of the target images. Due to the different thickness of components in concrete structures, external influences such as solar radiation cause temperature differences in the components depending on the component thickness (Figure 3).

Figure 4 is a model showing a unique temperature distribution under different thermal conditions, that is, detection in uniform temperature and detection with temperature gradient. If the temperature of the target structure is uniform, not only the amount of temperature change but also the size of the damage can be easily detected. However, in reality, the surface temperature of the target concrete structure has a significant temperature gradient due to the difference in component thickness, which makes it harder to detect damages than in stable temperature conditions.

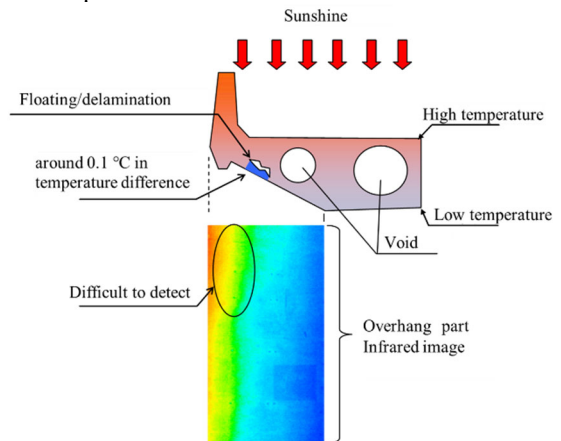


Figure 3. Thermal image example of RC hollow bridge with temperature difference

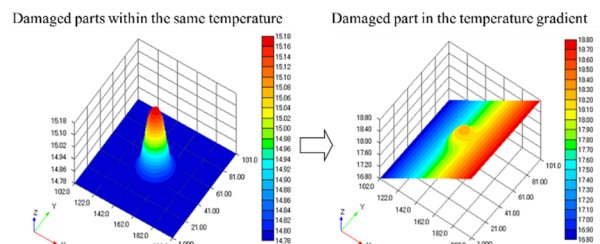


Figure 4. Concept of thermal change in the damaged area

In our study, to eliminate the influence of temperature gradient in concrete structures, we calculate the moving average of temperature distribution and subtract the target pixel temperature. It enables damage detection in concrete structures under the influence of temperature gradient; the detection result should be free from the temperature gradient in the target structures.

After the abovementioned preprocessing, we have constructed a system by machine learning to detect floating/delamination from thermal images. Machine learning requires training data, for which we collected through infrared thermography measurement, as well as the full-scale hammering tests on RC, steel and box-girder bridges that has been in service for 5 to 38 years. As for the infrared thermography, we conducted the measurement at night on the day when the diurnal range exceeded 10°C. Detecting singular temperature distribution with infrared thermography does not always mean the detection of floating/delamination. For instance, there are several factors that affect the temperature distribution of the target, such as free limes piled up by rainwater infiltration and roughness of the target surface itself. The following Table 2 shows the list of factors that cause temperature irregularity. Each is described in the following sections.

Table 2 Factors of temperature irregularity

Floating area
Delamination area
Adhered slag
Foreign substances
Repair marks
Free limes
Color irregularity

3.2 Factors of temperature irregularity

3.2.1 Floating area

The floating area, in this case, is an area where noise is generated in the hammering test, but the concrete surface is still intact. Comparing with the thermal image of the healthy area where a foreign object attached, the temperature distribution image on the floating area is not distinct.

3.2.2 Delamination area

The delaminating area, in this case, is an area where concrete flakes should fall when the hammering tests are conducted. Compared to the thermal image of the floating area, the image of this area distinctively shows a singular temperature distribution.

3.2.3 Adhered slag

The delaminating area, in this case, is an area where Slags remain on the joint form marks after the initial concrete placement turned to a thickness of 2-5 mm; thus, they are detected distinctively as thin linear singular temperature distributions that run along with

the joint form marks by infrared thermography.

3.2.4 Foreign substances

If foreign materials such as wood chips are mixed in the concrete of the covered components, they are detected as temperature irregularities by infrared thermography. Because the mortar plastered on top conceals the wood chips, it is impossible to detect from the visual image whether the foreign materials are mixed in it.

3.2.5 Repair marks

The standard repair procedure of the floating/delamination of concrete due to rebar corrosion is to remove that areas and fill the damaged sections with materials such as shrinkage-compensating mortar. If the thermal conductivity of the materials used for repair is different from that of concrete, they appear as singular temperature irregularities.

3.2.6 Free limes

Free limes adhering to the concrete surface appear as singular temperature irregularities in thermal detection. The difference in reflectance or thermal conductivity between free limes and healthy concrete surface or the existence of gaps in between free limes and concrete surface would be the cause of the detection.

3.2.7 Color irregularity

The color irregularity causes a singular temperature irregularity detection in the thermal image.

3.3 Full-Scale Hammering Test Results Summary

Figure 5 shows thermal images organized according to characteristics in detection shapes. We collated organized images with hammering test results to confirm significant characteristics in the shape of areas with singular temperature irregularity in the following five types; 1) delamination, 2) floating, 3) slag, 4) foreign substances, and 5) healthy area. Table 3 shows each characteristic. If we can calculate the value expressing the shape of the temperature irregularity area (shape features), we determined that it is possible to classify using these five types of machine learning.

Delamination	Floating	Slag	Foreign substances	Healthy area
Characteristic The surrounding shape is complex and red is off center	Characteristic The peripheral shape is smooth and the red center is in the middle	Characteristic The shape is long and narrow, and the surrounding shape is complicated	Characteristic Square shape, high red occupancy	Characteristic Yellow occupancy is high and red center of gravity is in the middle

Figure 5. Relationship between hammering test results and image processing

Table 3 Relationship between hammering test results and detection image shape characteristics

Sounding result	Unique temperature area shape characteristic	note
delamination	The red area is off the center of the whole area	Knock down
Abnormal sound only	The red area is at the center of the whole area	floating
foreign substances	Square shape, high red occupancy	False positive
slag(t=2~5mm)	The occupancy rate of red is high and the shape is square, but the periphery is more complicated than foreign substances	False positive
healthy area (Reflection)	High yellow area occupancy	False positive

3.4 Discrimination Index Using Geometrical Features in Thermal Images

In this study, we have examined the image filtering process that ternarizes the thermal images. Based on the emphasized index, we set the threshold values of ternarized red, yellow, and blue as follows; over 0.11 as red, over 0.08 and less than 0.11 as yellow, and over 0.04 and less than 0.08 as blue, respectively.

Considering the results in the previous section, the positional relationship between the red, yellow, and blue areas is important. If the red area appears near the center

of the blue area, the detected image is probably a floating area with abnormal sound alone. On the other hand, if the red area appears at the location apart from the center of the blue area, the detected area could be a delamination area. Thus, the distance between the centers of each area should be calculated as a feature for the discrimination index.

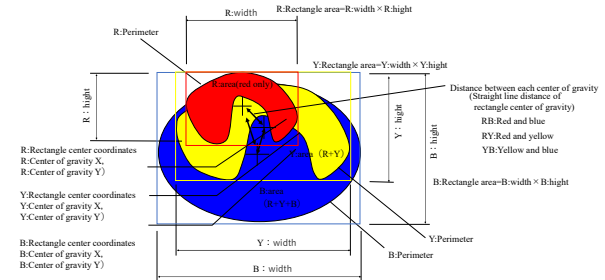


Figure 6. Concept of shape feature calculation of ternarized thermal images

The Shapes of red, yellow, and blue areas are also significant. In the thermal images of false detection, if its edge is smooth, it could be a floating area. Therefore, we examined shape features of red, yellow, and blue areas. The number of pixels represents circumference and dimension of the area. Occupancy rate, degree of shape complexity, and circularity level of each shape are calculated by the following equations, where L is the circumference and S is the area.

$$\text{Occupation rate (O)} = \frac{S}{R(\text{height}) \times R(\text{width})}$$

$$\text{Degree of shape complexity (C)} = \frac{L}{S} \quad (2)$$

$$\text{Circularity level (CL)} = \frac{4\pi A}{L^2}$$

In addition to the above values, we use the co-occurrence matrix[6][7][8], which is an image texture analysis method that can quantify changes in image contrast. The co-occurrence matrix firstly derives the matrix that uses the P-value of the target contrast in a specific position $\delta = (r, \theta)$ away from the point i should be the contrast j, $P\delta = (i, j)$, as its element (hereinafter referred to as stochastic matrix) to calculate several features by the matrix as shown in Figure 7. Values of the stochastic matrix represent frequency to each sample image, but practically we normalized them so that all numbers should be 1.

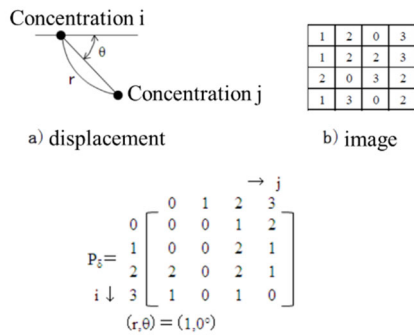


Figure 7. Co-occurrence matrix sample

We calculated following 14 features in total by the co-occurrence matrix mentioned above; Angular second moment, Contrast, Correlation, Sum of square variance, Inverse difference moment, Sum average, Sum variance, Sum entropy, Entropy, Difference variance, Difference entropy, Information measure of correlation 1, Information measure of correlation 2, Maximal correlation coefficient. We also set the position value δ as $r = 1, 2$ and the angle value θ as $0, 45, 90, 135, 180, 225,$ and 270 . As for the contrast, we set it in 32 levels of gray, and we generated the co-occurrence matrix.

3.5 Deep neural network

We used hammering test results as the training data for the deep neural network[9][10][11] developed in this study based on shape features obtained from analyzed images in the previous section. The shape features are ternarized areas, their positional relations, and those obtained by co-occurrence matrix. The data amount was 2,353 cases (hammering test results from 2008 to 2010).

In this study, a deep neural network with one input layer, six hidden layers, and one output layer was developed. The number of nodes in hidden layers are 453, 500, 600, 400, 300, and 100. The drop-out layer is also sandwiched between these layers. In this paper, the number of layers of the hidden layer for high accuracy is investigated by grid search. It is probably not the optimum value, but it is almost the optimum value and there is no problem in practical use.

4 RESULTS AND CONCLUSION

4.1 Results

Table 4 shows the accuracy of the deep neural network model. The overall accuracy was 88.7 % (2,086/2,353). In addition, 800 data which were not used for the learning were prepared, and the analysis by this method was carried out. As a result, Over 97% of the hammering results are in the top two of the

prediction results, which proves that this system is highly accurate.

Table 4 Analysis results of training dataset

sounding results \ analysis results	Delamination	Floating	Slag	Healthy area	Foreign substances	total
Delamination	111	2	0	32	2	147
Floating	2	116	2	12	0	132
Slag	1	0	34	6	0	41
Healthy area	64	71	17	1,732	42	1926
Foreign substances	3	0	0	11	93	107
total	181	189	53	1793	137	2353

4.2 Conclusion

It has been confirmed that the temperature gradient generated in the structure is removed by the image filtering process of the thermal image taken by the infrared camera, and the damage detection rate is improved. In addition, the image filtering process should be sufficient to deal with the influence of temperature differences around bridge appendages.

We also succeeded in building a deep neural network model that evaluates the presence and type of damage due to temperature changes. As inputs of deep neural network model, 14 feature quantities obtained from co-occurrence matrix, etc. were used. As a result, the accuracy of 88.7% was realized. Furthermore, the high accuracy was obtained even in the data set which was not used for the training. As a result of this study, floating/delamination can be remotely evaluated, which is considered to contribute to drastic improvement in efficiency of present inspection that depends on hammering sound.

5 Automatic detect system using a cloud server

5.1 Introduction of the system

Statistical analysis software is required to perform the damage detection described above, but such software can only be used by a limited number of users. Therefore, we have built a cloud server that can automate the damage detection for many users, and are currently conducting trial operations as shown in Fig. 8. This system is based on the machine learning system described above and can automatically detect damages based on infrared measurement and hammering test result data. Figure 9 shows an example of the use of an automatic detect system using a cloud server.

1. The thermal image (Figure 9(a)) is loaded into the analysis software “J-system” and ternarized areas, and their positional relations, and those obtained by

co-occurrence matrix are automatically output.

2. Upload the output to the cloud server.
3. Users download the results of the damage detection by the cloud server (Figure 9b).

The results of the infrared measurement are summarized in the above procedure. Figure 12c shows an example of delamination in a hammering test. This was the damage the proposed system determined to have a high probability of damage.

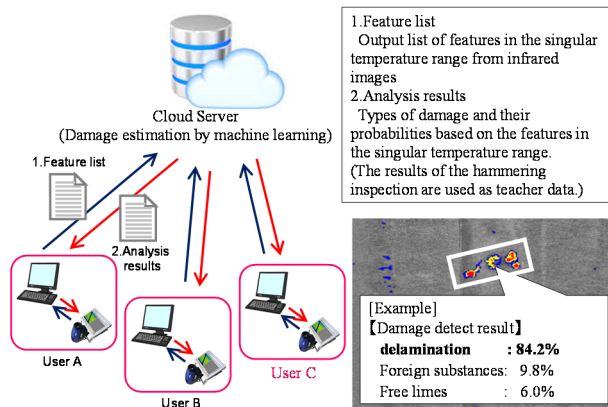
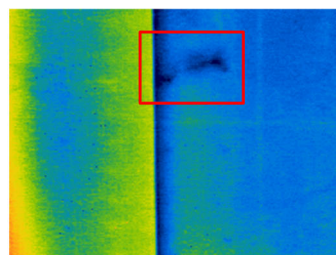
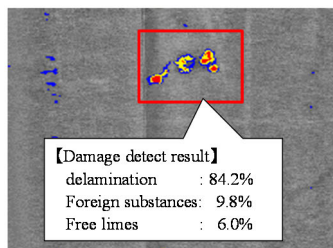


Figure 8. Automatic detect system using a cloud server



a) Infrared survey results: thermal images



b) Infrared survey results: Analytical images



c) Hammering test results: Remove floating

Figure 12. Example of Automatic detect Results from a Cloud Server

Utilizing a highly accurate system that automatically detects damages from infrared measurement results, the individual differences of surveyors are eliminated. The more data this system has, the more accurate the system will be at determining damages. When users of J-system perform the infrared survey and use the cloud server, the survey data will be stored on the cloud server, and as a result, the accuracy of the automatic detect system will be improved.

5.2 Introduction result

The J-system has been evaluated as a "non-destructive inspection technology that can detect floating and delamination of concrete structures" by the Bridge Maintenance Subcommittee of the Committee for Verification of Robots for Next Generation Infrastructure.

In addition, the J-system has been installed in the Shikoku branch of NEXCO West Japan since 2008 as a hammering sound screening system for periodic bridge inspections. It has also been used by NEXCO Central Japan, NEXCO East Japan, and Honshu-Shikoku Bridge Expressway, and has been introduced on a trial basis on bridges owned by the national government since fiscal 2015. The total survey area that West Nippon Expressway Engineering Shikoku Co., Ltd. received an order for is 2.55 million square meters (as of the end of FY2017). We will continue to develop a high-precision infrared measurement system so that it can be widely used for bridge inspection and surveys, including prevention of damage to third parties.

References

- [1] Cheng, L., & Tian, G. Y. 2012. Comparison of nondestructive testing methods on detection of delaminations in composites. *Journal of sensors*, 2012.
- [2] Oh, T., Kee, S. H., Arndt, R. W., Popovics, J. S., & Zhu, J. 2012. Comparison of NDT methods for assessment of a concrete bridge deck. *Journal of Engineering Mechanics*, 139(3), 305-314.
- [3] ASTM. 2007. Standard test method for detecting delaminations in bridge decks using infrared thermography. *ASTM D 4788*.
- [4] Kimura, T., Zhang, T., & Fukuda, H. 2019. A Proposal for the Development of a Building Management System for Extending the Lifespan of Housing Complexes in Japan. *Sustainability*, 11-(20), 5622.
- [5] Plesu, R., Teodoriu, G., & Taranu, G. 2012. Infrared thermography applications for building investigation. *Buletinul Institutului Politehnic Din Lasii. Sectia Constructii, Arhitectura*, 58(1), 157.
- [6] Chun, P., Funatani, K., Furukawa, S., & Ohga, M.

2013. Grade classification of corrosion damage on the surface of weathering steel members by digital image processing, In *Proceedings of the Thirteenth East Asia-Pacific Conference on Structural Engineering and Construction (EASEC-13)* (pp. G-4). The Thirteenth East Asia-Pacific Conference on Structural Engineering and Construction (EASEC-13).
- [7] Partio, M., Cramariuc, B., Gabbouj, M., & Visa, A. 2002. Rock texture retrieval using gray level co-occurrence matrix. In *Proc. of 5th Nordic Signal Processing Symposium* (Vol. 75).
- [8] Pathak, B., & Barooah, D. (2013). Texture analysis based on the gray-level co-occurrence matrix considering possible orientations. *International Journal of Advanced Research in Electrical, Electronics and Instrumentation Engineering*, 2(9), 4206-4212.
- [9] LeCun, Y., Bengio, Y., & Hinton, G. 2015. Deep learning. *nature*, 521(7553), 436-444.
- [10] Sainath, T. N., Mohamed, A. R., Kingsbury, B., & Ramabhadran, B. 2013. Deep convolutional neural networks for LVCSR. In *2013 IEEE international conference on acoustics, speech and signal processing* (pp. 8614-8618). IEEE.
- [11] Simões, N., Simões, I., Tadeu, A., & Serra, C. 2012. Evaluation of adhesive bonding of ceramic tiles using active thermography. In *Proceedings of 11th Quantitative InfraRed Thermography conference, paper QIRT2012-362, Naples (Italy)*.